

Wireless Positioning Method Based on Back Propagation Neural Network with TOA Measurement

Chien-Sheng Chen¹, Jen-Fa Huang², Guo-Ren Shia³

¹Department of Information Management, Tainan University of Technology, Tainan, Taiwan

^{2,3}Department of Electrical Engineering, National Cheng Kung University, Tainan, Taiwan

Abstract: Cellular mobile communication system has been widely applied in mobile communication. The usual methods utilize the base stations (BS) to position the target mobile station (MS). In this research, we employ inverse matrices to calculate the values of weighted geometric dilution of precision (WGDOP) with the subsets of the BSs. The BS subset which owns the minimum value of WGDOP should have the higher precision of locating the mobile station. Then, we propose the method of positioning the mobile station with back propagation neural network (BPNN). In this proposed scheme, we should obtain the training data first. Next, it needs to classify the several classes from training data, confirm the input information and construct the corresponding architectures of neural network with those classes. After training stage, the evaluation of trained model with the testing data is necessary. In the simulation results, we compare the residuals of the BS sets of the three smallest values of WGDOP and the performances of the positioning method with BPNN and other algorithms.

Keywords: Mobile Communication System, Weighted Geometric Dilution of Precision (WGDOP), Artificial neural network (ANN), Time of arrival (TOA).

Date of Submission: 22-03-2020

Date of Acceptance: 09-04-2020

I. Introduction

Due to increasing of mobile devices, local base services become a popular issue in mobile communication. Thus, lots of schemes for positioning have been published such as angle of arrival (AOA) [1], time of arrival (TOA) [2][3], time differences of arrival (TDOA) [4][5], received signal strength (RSS) [6]. Cellular Communication System [7][8] consists of the center base station, the six nearest base stations and the mobile station. When the mobile station locates in the cell of the base station, that base station is called serving base station. It means that the serving base station has the lowest measurement error because it is closer the mobile station than other base stations.

Weighted geometric dilution of precision [9] has been applied to evaluate the performance of the sets of satellites in global positioning system (GPS). If the value of WGDOP is smallest, the corresponding set of satellites has the best distribution in geometric relation. Nowadays, lots of intelligent algorithms for artificial neural network are published, such as gradient descent (GD), scaled conjugate gradient (SCG) [10], resilient back-propagation (Rprop) [11], and Levenberg-Marquardt (LM).

In this study, we will construct the environment for simulating the cellular communication. It consists of the seven BSs, and the MS will generate randomly in the area of the serving BS. Then, we will pick up the best set of the three BSs and the serving station by calculating the WGDOP values of all the sets. Afterwards, we can obtain the TOA information from the MS and the four BSs. With the distance information and the positions of the four BSs, the four circular equations will be derived. The MS must locate at the intersection range of the four circles.

This paper proposed the method that uses Levenberg-Marquardt Algorithm in neuron network to estimate the location of the MS. The corresponding inputs will be the coordinates of the intersection points of the four BSs circles. And the outputs of the neural network are the coordinates of the MS in estimation.

II. Weighted geometric dilution of precision

Geometric dilution of precision (GDOP) [12] is used to judge the geometry of measurement units, like satellites in GPS. The value of GDOP is calculated by the factors of distance in dimensions and time delay. The calculation of GDOP can apply to n-dimension environment scenario. For example, the distance in the 2-D Cartesian environment between the MS and the i -th BS can be expressed below.

$$r_i = \sqrt{(X_i - x)^2 + (Y_i - y)^2} + v_i + c \times t_s \quad (1)$$

where (x, y) denotes the position of the MS, and (X_i, Y_i) denotes the i -th measurement unit, such as satellite in GPS or base station in cellular communication system. v_i is pseudo-range measurements noise, c is the speed of light, and t_s is time shift.

Define the location nearby the MS to be (\hat{x}, \hat{y}) . The distance between (\hat{x}, \hat{y}) and the i -th BS can be expressed as equation (2).

$$\hat{r}_i = \sqrt{(X_i - \hat{x})^2 + (Y_i - \hat{y})^2} \tag{2}$$

Equation (2) can be rewritten as Equation (3) by Taylor series expansion.

$$\hat{r}_i = \sqrt{(X_i - x)^2 + (Y_i - y)^2} - e_{ix} \cdot \delta_x - e_{iy} \cdot \delta_y \tag{3}$$

$$e_{ix} = \frac{\hat{x} - X_i}{\hat{r}_i}, e_{iy} = \frac{\hat{y} - Y_i}{\hat{r}_i}$$

where δ_x and δ_y are offsets between the MS (x, y) and (\hat{x}, \hat{y}) in the 2-D Cartesian environment.

Then, the residual Δr_i between \hat{r}_i and r_i will be derived as the following

$$\Delta r_i = r_i - \hat{r}_i = e_{ix} \cdot \delta_x + e_{iy} \cdot \delta_y + v_i + c \times t_s \tag{4}$$

The relationship for all n measurement units can be linearized from eq. (4):

$$z = H\delta + V \tag{5}$$

$$z = \begin{bmatrix} r_1 - \hat{r}_1 \\ r_2 - \hat{r}_2 \\ \vdots \\ r_n - \hat{r}_n \end{bmatrix}, H = \begin{bmatrix} e_{1x} & e_{1y} & 1 \\ e_{2x} & e_{2y} & 1 \\ \vdots & \vdots & \vdots \\ e_{nx} & e_{ny} & 1 \end{bmatrix}, \delta = \begin{bmatrix} \delta_x \\ \delta_y \\ c \cdot t_s \end{bmatrix}, V = \begin{bmatrix} v_1 \\ v_2 \\ \vdots \\ v_n \end{bmatrix}$$

We can utilize the linear least squares (LLS) method to estimate the solution $\hat{\delta}_{LLS}$. It is given by

$$\hat{\delta}_{LLS} = (H^T H)^{-1} H^T z \tag{6}$$

If the pseudo-range errors of all n measurement units are uncorrelated and there has the same variance σ^2 for them. The covariance matrix is expressed as the equation (7).

$$E[(\hat{\delta}_{LLS} - \delta)(\hat{\delta}_{LLS} - \delta)^T] = \sigma(H^T H)^{-1} \tag{7}$$

$$\sigma = \begin{bmatrix} \sigma_1^2 & 0 & \dots & 0 \\ 0 & \sigma_2^2 & \dots & 0 \\ \vdots & \vdots & \ddots & \vdots \\ 0 & 0 & \dots & \sigma_n^2 \end{bmatrix}, \sigma_1^2 = \sigma_2^2 = \dots = \sigma_n^2 = \sigma^2$$

Because of the same variance for n measurement units, the GDOP value is computed by the equation (8) below:

$$GDOP = \sqrt{\text{tr}((H^T H)^{-1})} \tag{8}$$

In the real environment, there are different variances in several measurement units. Thus, it is necessary to derive the form of weighted geometric dilution of precision (WGDOP). We applied the weighted least squares (WLS) method to estimate the solution for this case.

$$\hat{\delta}_{WLS} = (H^T W H)^{-1} H^T W z \tag{9}$$

where W denotes the matrix that consists of the reciprocals of variances corresponding to measurement units, respectively.

$$W = \begin{bmatrix} 1/(\sigma_1^2) & 0 & \dots & 0 \\ 0 & 1/(\sigma_2^2) & \dots & 0 \\ \vdots & \vdots & \ddots & \vdots \\ 0 & 0 & \dots & 1/(\sigma_n^2) \end{bmatrix} \tag{10}$$

The covariance matrix for WLS can be rewritten by the equation (5) and equation (9). It shows as

$$E[(\hat{\delta}_{WLS} - \delta)(\hat{\delta}_{WLS} - \delta)^T] = (H^T W H)^{-1} \tag{11}$$

According to the equation (11), the WGDOP value is defined as

$$WGDOP = \sqrt{\text{tr}((H^T W H)^{-1})} \tag{12}$$

If the subset A of the measurement units has the smallest value of WGDOP besides all the subsets, it means that the subset A has the best geometry for positioning.

III. Positioning in TOA trilateration method

Due to the impact of non-light-of-sight (NLOS) errors, the measurement distance R_i from the i -th BS to the MS is larger than the true distance r_i . It causes that there is the overlap with the three BSs as shown Figure 1, but not an intersection point.

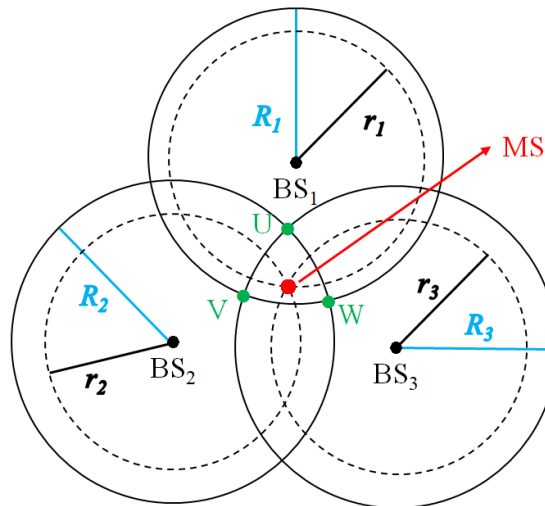


Fig. 1. TOA Trilateration with NLOS error and without NLOS error

Therefore, lots of TOA positioning algorithms were applied to achieve the optimal estimation location with the least location error. Derive the intersection points from any pair of two BS circles and pick up those points which locate in the overlap of the three circles. For example, the points U, V, W are shown as Figure 1. Assume that there are three points as the vertices of the intersection area. Several methods use the geometry of the three measurement circles for estimating the position of the MS.

(i) Averaging method

The average method utilizes the vertices U, V, W of the intersection area to gain the solution (\hat{x}_N, \hat{y}_N) expressed by the formula (13).

$$\hat{x}_N = \frac{x_U + x_V + x_W}{3}, \hat{y}_N = \frac{y_U + y_V + y_W}{3} \tag{13}$$

(ii) Distance-weighted method

The weights of the points U, V, W are the core concept in this method. First, we will calculate the distance d_i from the point U, V, W to the averaging point (\hat{x}_N, \hat{y}_N) derived by equation (13).

$$d_i = \sqrt{(x_i - \hat{x}_N)^2 + (y_i - \hat{y}_N)^2}, i = U, V, W \tag{14}$$

The estimation location of the MS will be determined by the following formula.

$$\begin{cases} \hat{x}_d = \frac{\frac{1}{d_U} \times x_U + \frac{1}{d_V} \times x_V + \frac{1}{d_W} \times x_W}{\frac{1}{d_U} + \frac{1}{d_V} + \frac{1}{d_W}} \\ \hat{y}_d = \frac{\frac{1}{d_U} \times y_U + \frac{1}{d_V} \times y_V + \frac{1}{d_W} \times y_W}{\frac{1}{d_U} + \frac{1}{d_V} + \frac{1}{d_W}} \end{cases} \tag{15}$$

The point closer to the averaging point will take the larger weight for estimating the MS.

(iii) Taylor series algorithm (TSA)

In this method [13][14], define the true position of the MS is (x, y) and we should generate the initial estimation location of the MS as (x_v, y_v) . The relationship of (x, y) and (x_v, y_v) can be expressed as

$$\begin{aligned} x &= x_v + \delta_{vx} \\ y &= y_v + \delta_{vy} \end{aligned}, i = 1, 2, 3 \tag{16}$$

$$r_{vi} = \sqrt{(X_i - x_v)^2 + (Y_i - y_v)^2}$$

where $(\delta_{vx}, \delta_{vy})$ denotes the residual of the estimation and the true position. And (X_i, Y_i) is the coordination of the i -th BS.

The true radius of the i -th BS can be linearized by equation (16) as the following equations.

$$r_i \cong r_{vi} + a_{ix} \cdot \delta_{vx} + a_{iy} \cdot \delta_{vy}, i = 1, 2, 3 \tag{17}$$

$$\text{where } a_{ix} = \left. \frac{\partial r_i}{\partial x} \right|_{x_v, y_v}, a_{iy} = \left. \frac{\partial r_i}{\partial y} \right|_{x_v, y_v}$$

Equation (17) can be rewritten as

$$A\delta \cong Z \tag{18}$$

$$\text{where } A = \begin{bmatrix} a_{1x} & a_{1y} \\ a_{2x} & a_{2y} \\ a_{3x} & a_{3y} \end{bmatrix}, \delta = \begin{bmatrix} \delta_x \\ \delta_y \end{bmatrix}, z = \begin{bmatrix} r_1 - r_{v1} \\ r_2 - r_{v2} \\ r_3 - r_{v3} \end{bmatrix}$$

The residual vector δ can be solved by the linear least square method as the equation below.

$$\delta = (A^T A)^{-1} A^T z \tag{19}$$

In this method, the estimation position will be updated iteratively until the residual δ reaches the minimum.

IV. Neural network and Levenberg-Marquardt algorithm

The technique of neural network has been developing in recent decades. It is widely used to solve the classification problems and the optimization problems. The traditional architecture of neural network is made of the three types of layers: input layer, hidden layers and output layer. These layers consist of numerous neurons and there are weight links and biases between each neuron in the different layer, such as input layer to hidden layer, hidden layer to hidden layer, or hidden layer to output layer. The architecture is shown as Figure 2 below. The number of neurons in the input layer and the output layer corresponds to the input factors and the quantity of outputs in the problem to be solved.

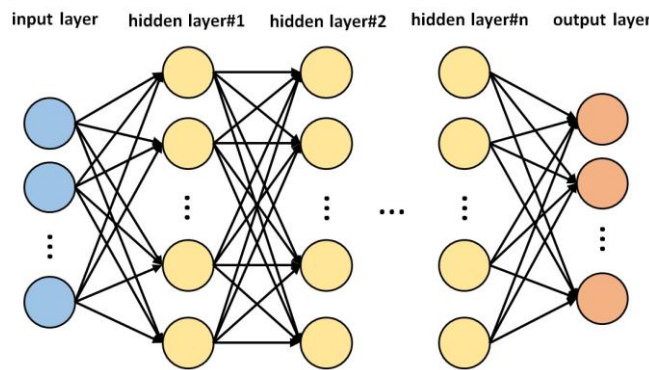


Fig. 2. Structure of neural network

In the training stage, the error function E is sum square error function, and it is defined as

$$E = \frac{1}{2} \sum_{l=1}^L \sum_{m=1}^M (e_{l,m})^2 \tag{20}$$

where L denotes the number of observations, and M is the number of the output nodes. e is the error of the output vector.

$$e_{l,m} = t_{l,m} - y_{l,m} \tag{21}$$

where t is defined as the target output vector and y is the observed output vector.

In the gradient descent method, the definition of gradient \mathbf{g} can be expressed as

$$\mathbf{g} = \frac{\partial E}{\partial \mathbf{w}} = \left[\frac{\partial E}{\partial w_1} \quad \frac{\partial E}{\partial w_2} \quad \dots \quad \frac{\partial E}{\partial w_N} \right]^T \tag{22}$$

where \mathbf{w} denotes the weight vector with N weights. Then, the update rule of the gradient descent method is the equation below.

$$w_{k+1} = w_k - \alpha \cdot g_k \tag{23}$$

where α is the constant of learning rate. Gauss-Newton method utilizes Jacobian matrix J to construct the rule of weight updating.

$$w_{k+1} = w_k - (J_k^T J_k)^{-1} J_k^T e_k \tag{24}$$

$$J = \begin{bmatrix} \frac{\partial e_{1,1}}{\partial w_1} & \frac{\partial e_{1,1}}{\partial w_2} & \dots & \frac{\partial e_{1,1}}{\partial w_N} \\ \frac{\partial e_{1,2}}{\partial w_1} & \frac{\partial e_{1,2}}{\partial w_2} & \dots & \frac{\partial e_{1,2}}{\partial w_N} \\ \vdots & \vdots & \vdots & \vdots \\ \frac{\partial e_{L-1,M}}{\partial w_1} & \frac{\partial e_{L-1,M}}{\partial w_2} & \dots & \frac{\partial e_{L-1,M}}{\partial w_N} \\ \frac{\partial e_{L,1}}{\partial w_1} & \frac{\partial e_{L,1}}{\partial w_2} & \dots & \frac{\partial e_{L,1}}{\partial w_N} \\ \vdots & \vdots & \vdots & \vdots \\ \frac{\partial e_{L,M}}{\partial w_1} & \frac{\partial e_{L,M}}{\partial w_2} & \dots & \frac{\partial e_{L,M}}{\partial w_N} \end{bmatrix}, e = \begin{bmatrix} e_{1,1} \\ e_{1,2} \\ \vdots \\ e_{L-1,M} \\ e_{L,1} \\ \vdots \\ e_{L,M} \end{bmatrix}$$

The Levenberg-Marquardt (LM) algorithm [15] combined the gradient descent method and Gauss-Newton method. To guarantee that the Hessian matrix $J^T J$ is invertible, LM achieved the Hessian matrix by another form. The rule of weights updating is expressed as:

$$w_{k+1} = w_k - (J_k^T J_k + \mu I)^{-1} J_k^T e_k \tag{25}$$

where μ denotes the constant of adapting learning, and it is given as positive value. I is the identity matrix. When μ decreases to nearly zero, the learning method will approach to Gauss-Newton method. If μ becomes greatly large, LM approximates to the gradient descent method and μ will be the constant of learning rate shown as equation (26).

$$\mu = \frac{1}{\alpha} \tag{26}$$

V. Neural network architecture for positioning

We proposed the scheme of positioning with BPNN in this paper. In Section II, we select the best subset from all the BSs by computing the values of WGDOP. Then, we can obtain the measuring circles by the positions of BSs and individual measurement distances. For example, if the subset that includes BS₁, BS₂, BS₄ and BS₆ is the best subset, and it is shown as Figure 3 for the four BSs. We will utilize the coordination of the vertices of the intersection area as the inputs of the model. The true position of the MS is set as the output of the model.

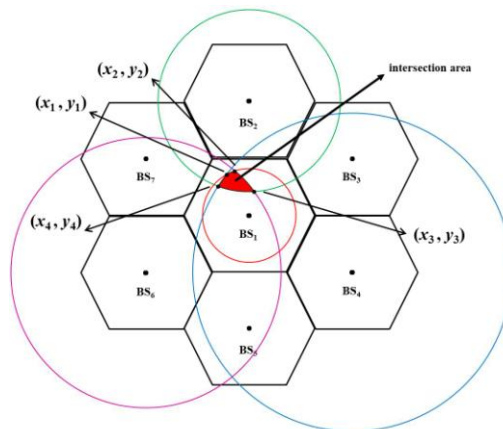


Fig. 3. The four base stations with the minimum WGDOP in the cellular communication system

In our proposed scheme, we will train the two model of x and y in the 2-D Cartesian environment. At first, we should collect amounts of training data. Then, there are several types of data with different numbers of inputs. In other words, the number of vertices of the intersection area is not only four in all the scenarios. In other cases, there will be different numbers of vertices in the overlap. So, we should gather enough data to train the models of any possible situations. The architecture of the two models of x and y is shown in Fig 4.

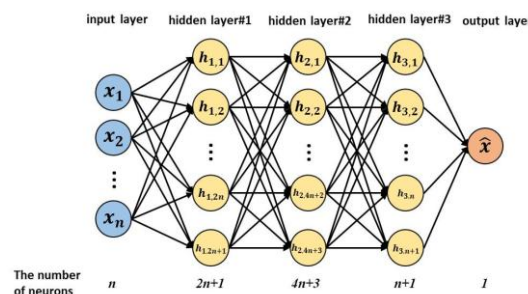


Fig. 4(a). Structure of the model for estimating the coordination of x of the MS.

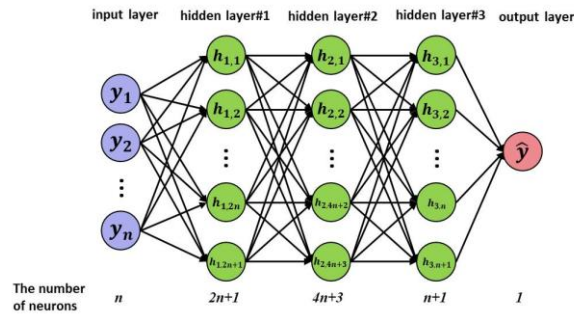


Fig. 4(b). Structure of the model for estimating the coordination of y of the MS.

where (x_i, y_i) denotes the coordination of the i -th vertex of the intersection area, and (\hat{x}, \hat{y}) is the estimation location of the MS. In this paper, we use three hidden layers to construct the model. The tan-sigmoid function is used to be activation functions in the first and second hidden layer. The third one links to the output layer with pure linear function as activation function.

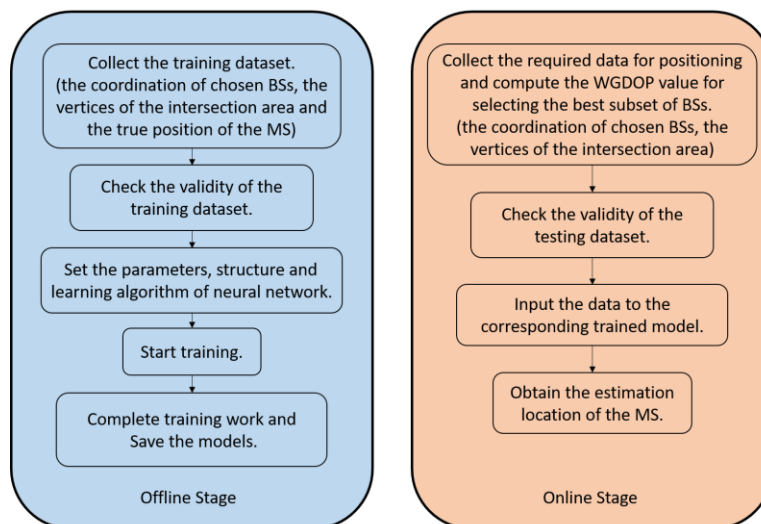


Fig. 5. Flow chart of offline stage and online stage

VI. Simulation Results

In order to evaluate the performance of proposed method and other methods, we construct the environment with the cellular mobile communication system to simulate the position of the MS. In our scenario, we set the BSs as $(0m, 0m)$, $(0m, 5000m)$, $(2500\sqrt{3}m, 2500m)$, $(2500\sqrt{3}m, -2500m)$, $(0m, -5000m)$, $(-2500\sqrt{3}m, -2500m)$, $(-2500\sqrt{3}m, 2500m)$. The MS will generate at the cell of the BS_1 with uniform distribution. It is shown as Figure 6.

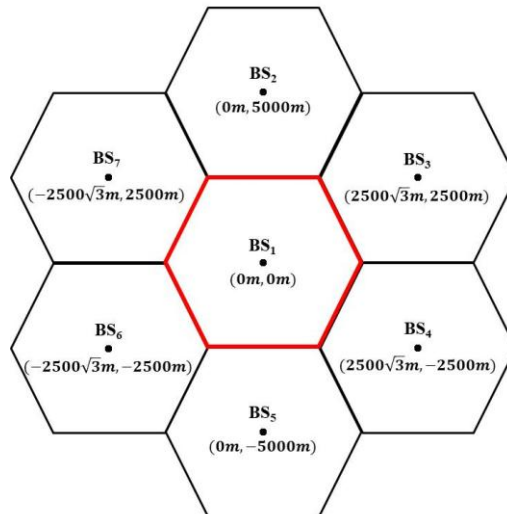


Fig. 6. The cellular wireless communication system in simulations.

We generated the 10000 samples and calculate the WGDOP value for each one. In the selection of BSs subsets, we use the four BSs in a subset. Because the MS always locates at the cell of the BS₁, we choose the BS₁ in each subset. Thus, there are $C(6,3) = 20$ subsets in each sample. For the accurate estimation of the MS, we chose the subset with the minimum WGDOP to position the MS.

In our simulations, there are the five situations with the two vertices to six vertices in the overlap of the four BSs circles.

Number of vertices	2	3	4	5	6	total
Counts of Samples	9	1846	8111	33	1	10000

Table 1. The statistical results of number of vertices and counts of samples.

In general, the cases with three or four vertices occupy all the results. Therefore, we trained the two models of x and y with 10000 samples for each one. The evaluation of performance with BPNN and other algorithms for 10000 times positioning is shown as Figure 7.

In the case with three vertices, all the location error of simulations with BPNN is lower than 210m. The averaging method, distance weight method and TSA are at least two times larger than BPNN. In another case for four vertices, the performance of positioning with BPNN is still better than other methods.

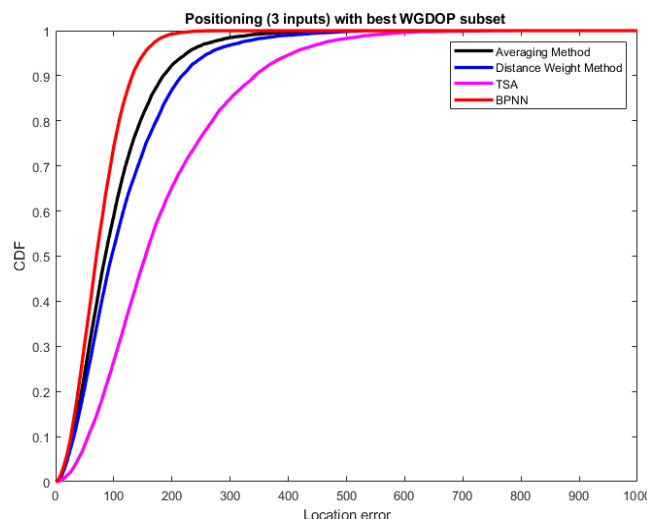


Fig. 7(a). The CDF of location error with BPNN and other algorithms for the case with 3 inputs.

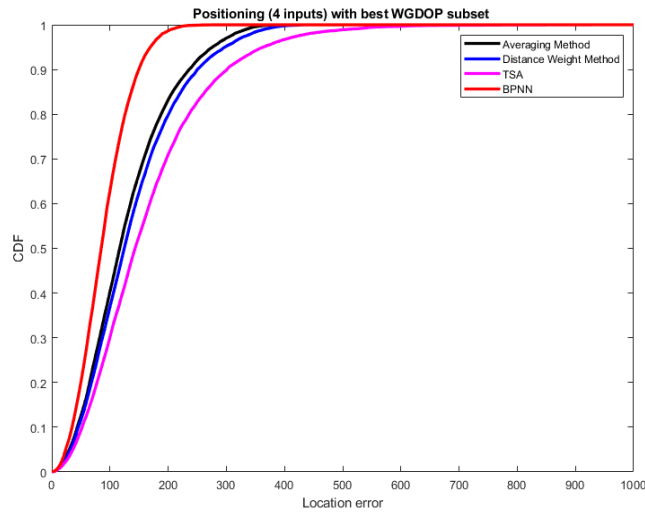


Fig. 7(b). The CDF of location error with BPNN and other algorithms for the case with 4 inputs.

Next, we verified the performance of selecting different BSs subsets with worse WGDOP value. In the next simulation results, we utilized the BSs subsets with the smallest, the secondsmallest and the thirdsmallest value of WGDOP for positioning. The simulation results are shown as Figure 8.

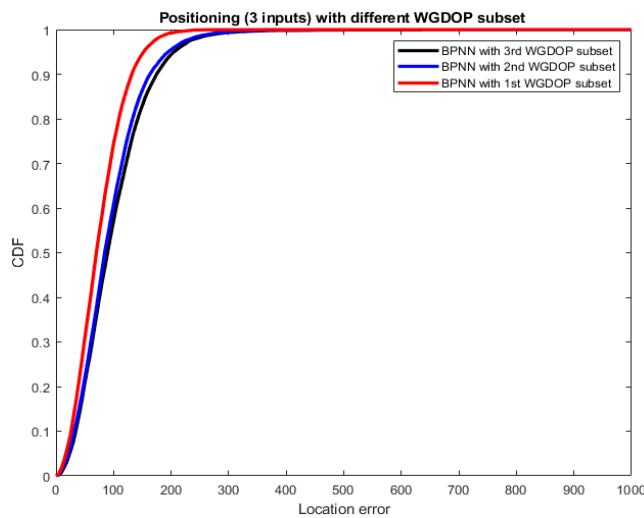


Fig. 8(a). The CDF of location error with different BSs subsets for the case with 3 inputs.

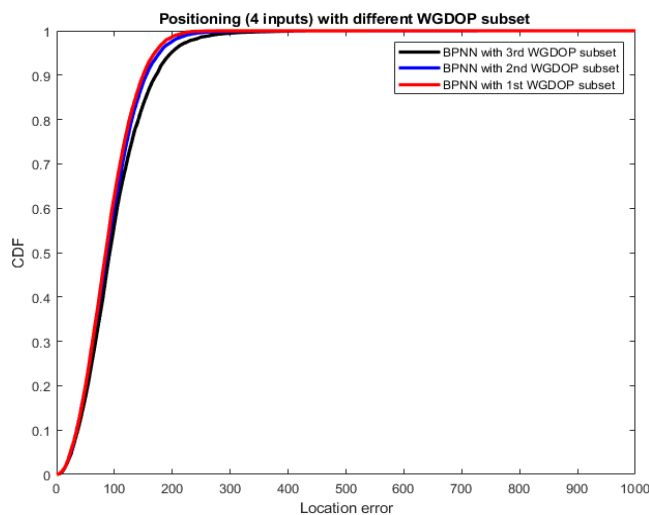


Fig. 8(b). The CDF of location error with different BSs subsets for the case with 4 inputs.

In Figure 8, the location error of the BSs subset with the smallest WGDOP value is lower than the others. It indicates that the higher accurate positioning is correlated with the smaller value of WGDOP. Thus, selecting the best subset from all the measurement units is effective to raise the performance of positioning.

VII. Conclusions

In this paper, we validated the importance of selecting the subset by WGDOP value. Before positioning work, we can choose the best subsets by calculating the WGDOP values for optimal positing performance. It is effective to reduce the complexity of computing and remain the higher accuracy.

We have proposed a scheme using the BPNN for positioning the mobile station by several sensors or measurement units. We set the coordination of vertices in the overlap of the selected measurement circles as the inputs. According to various situations of intersection points, we should establish multiple models corresponded to the number of vertices. In the simulation results, it is confirmed that the performance of the proposed method is better than averaging method, distance weight method and TSA. The architecture for positioning can apply to the communication systems, such as wireless sensor network, cellular wireless communication system or geometric precision system.

Acknowledgements

This research was supported in part by Higher Education Sprout Project, Ministry of Education to the Headquarters University Advancement at National Cheng Kung University (NCKU).

References

- [1]. Rong, P., & Sichertiu, M. L. (2006, September). "Angle of arrival localization for wireless sensor networks." In *2006 3rd annual IEEE communications society on sensor and ad hoc communications and networks* (Vol. 1, pp. 374-382). IEEE.
- [2]. Venkatraman, S., Caffery, J., & You, H. R. (2004). "A novel TOA location algorithm using LOS range estimation for NLOS environments." *IEEE Transactions on Vehicular Technology*, 53(5), 1515-1524.
- [3]. Guvenc, I., & Chong, C. C. (2009). "A survey on TOA based wireless localization and NLOS mitigation techniques." *IEEE Communications Surveys & Tutorials*, 11(3), 107-124.
- [4]. Mensing, C., Plass, S., "Positioning algorithms for cellular networks using TDOA." *Proceedings of the 2006 IEEE International Conference on Acoustics, Speech and Signal Processing, ICASSP 2006*, vol. 4 (May 2006)
- [5]. Qu, X., Xie, L., & Tan, W. (2017). "Iterative constrained weighted least squares source localization using TDOA and FDOA measurements." *IEEE Transactions on Signal Processing*, 65(15), 3990-4003.
- [6]. Chen, X., Edelstein, A., Li, Y., Coates, M., Rabbat, M., & Men, A. (2011, April). "Sequential Monte Carlo for simultaneous passive device-free tracking and sensor localization using received signal strength measurements." In *Proceedings of the 10th ACM/IEEE International Conference on Information Processing in Sensor Networks* (pp. 342-353). IEEE.
- [7]. Wang, C. X., Haider, F., Gao, X., You, X. H., Yang, Y., Yuan, D., ... & Hepsaydir, E. (2014). "Cellular architecture and key technologies for 5G wireless communication networks." *IEEE communications magazine*, 52(2), 122-130.
- [8]. Ge, X., Tu, S., Mao, G., Wang, C. X., & Han, T. (2016). "5G ultra-dense cellular networks." *IEEE Wireless Communications*, 23(1), 72-79.
- [9]. Sairo, H., Akopian, D., & Takala, J. (2003). "Weighted dilution of precision as quality measure in satellite positioning." *IEEE Proceedings-Radar, Sonar and Navigation*, 150(6), 430-436.
- [10]. Moller, M. F. (1993). "A scaled conjugate gradient algorithm for fast supervised learning." *Neural networks*, 6(4), pp.525-533.
- [11]. Riedmiller, M., & Braun, H. (1993, March). "A direct adaptive method for faster backpropagation learning: The RPROP algorithm." In *Proceedings of the IEEE international conference on neural networks* (Vol. 1993, pp. 586-591).
- [12]. Xue, S., & Yang, Y. (2015). "Positioning configurations with the lowest GDOP and their classification." *Journal of geodesy*, 89(1), 49-71.
- [13]. Wang, Z., Ye, N., Malekian, R., Xiao, F., & Wang, R. (2016). "TrackT: Accurate tracking of RFID tags with mm-level accuracy using first-order Taylor series approximation." *Ad hoc networks*, 53, 132-144.
- [14]. Caffery J. "A new approach to the geometry of TOA location." *Proceedings of the 52nd IEEE vehicular technology conference (IEEE-VTS Fall VTC 2000)*, Boston, MA, 24-28 September 2000, (Vol. 4, pp.1943-1949).
- [15]. Sapna, S., Tamilarasi, A., & Kumar, M. P. (2012). "Backpropagation learning algorithm based on Levenberg Marquardt Algorithm." *Comp Sci Inform Technol (CS and IT)*, 2, 393-398.